


Article

Benthic Foraminiferal Assemblages and Rhodolith Facies Evolution in Post-LGM Sediments from the Pontine Archipelago Shelf (Central Tyrrhenian Sea, Italy)

Virgilio Frezza ^{1,*}, Letizia Argenti ², Andrea Bonifazi ³, Francesco L. Chiocci ¹, Letizia Di Bella ¹ , Michela Ingrassia ⁴ and Eleonora Martorelli ⁴

¹ Dipartimento di Scienze della Terra, Sapienza Università di Roma, P. le A. Moro, 5, 00185 Rome, Italy; francesco.chiocci@uniroma1.it (F.L.C.); letizia.dibella@uniroma1.it (L.D.B.)

² Independent Researcher, Via Clarice Tartufari, 161, 00128 Rome, Italy; letizia.argenti2020@gmail.com

³ Dipartimento di Biologia, Università di Roma “Tor Vergata”, 00133 Rome, Italy; bonifazi.andrea@virgilio.it

⁴ CNR-IGAG (Istituto di Geologia Ambientale e Geoingegneria), UOS Roma, P. le A. Moro, 5, 00185 Rome, Italy; michela.ingrassia@cnr.it (M.I.); eleonora.martorelli@cnr.it (E.M.)

* Correspondence: vfrezza@gmail.com

Abstract: The seabed of the Pontine Archipelago (Tyrrhenian Sea) insular shelf is peculiar as it is characterized by a mixed siliciclastic–carbonate sedimentation. In order to reconstruct the Late Quaternary paleoenvironmental evolution of the Pontine Archipelago, this study investigates the succession of facies recorded by two sediment cores. For this purpose, benthic foraminifera and rhodoliths assemblages were considered. The two cores (post-Last Glacial Maximum in age) were collected at 60 (CS1) and 122 m (Caro1) depth on the insular shelf off Ponza Island. The paleontological data were compared with seismo-stratigraphic and lithological evidence. The cores show a deepening succession, with a transition from a basal rhodolith-rich biodetritic coarse sand to the surface coralline-barren silty sand. This transition is more evident along core Caro1 (from the bottom to the top), collected at a deeper water depth than CS1. In support of this evidence, along Caro1 was recorded a fairly constant increase in the amount of planktonic foraminiferal and a marked change in benthic foraminiferal assemblages (from *Asterigerinata mamilla* and *Lobatula lobatula* assemblage to *Cassidulina carinata* assemblage). Interestingly, the dating of the Caro1 bottom allowed us to extend to more than 13,000 years BP the rhodolith record in the Pontine Archipelago, indicating the possible presence of an active carbonate factory at that time.

Keywords: benthic foraminifera; coralline red algae; paleoenvironmental reconstruction; late quaternary; Pontine Archipelago; Tyrrhenian sea



Citation: Frezza, V.; Argenti, L.; Bonifazi, A.; Chiocci, F.L.; Di Bella, L.; Ingrassia, M.; Martorelli, E. Benthic Foraminiferal Assemblages and Rhodolith Facies Evolution in Post-LGM Sediments from the Pontine Archipelago Shelf (Central Tyrrhenian Sea, Italy). *Geosciences* **2021**, *11*, 179. <https://doi.org/10.3390/geosciences11040179>

Academic Editors: Jesus Martinez-Frias and Angelos G. Maravelis

Received: 26 February 2021

Accepted: 14 April 2021

Published: 16 April 2021

Publisher's Note: MDPI stays neutral with regard to jurisdictional claims in published maps and institutional affiliations.



Copyright: © 2021 by the authors. Licensee MDPI, Basel, Switzerland. This article is an open access article distributed under the terms and conditions of the Creative Commons Attribution (CC BY) license (<https://creativecommons.org/licenses/by/4.0/>).

1. Introduction

In non-tropical shelf areas (such as the western Mediterranean), when the terrigenous input rate is low (lower than 10 mm per 1000 years; [1]), extensive deposits of skeletal carbonates may accumulate [2]. Non-tropical carbonate sediments are composed almost entirely of heterozoan skeletal remains (sensu [3]) represented by benthic foraminifera, bryozoans, bivalves, barnacles and coralline red algae, constituting foramol-rhodalgal associations (e.g., [4]).

The Mediterranean area is normally characterized by terrigenous sedimentation derived from fluvial inputs and erosional coastal processes; nonetheless, examples of modern shelf carbonate production are present [5–8], for example, in sectors far from main river mouths (e.g., insular shelves around islands) or off karstic coastal regions. In the Italian seas, carbonate deposition occurs in the southern Adriatic Sea, Cagliari Bay (Sardinia), Adventure Bank (southwestern Sicily), Gulf of Naples and Pontine Archipelago [2,9–16].

Several studies investigated seabed carbonate sediment from the Pontine Archipelago (Tyrrhenian Sea), focusing on sedimentary features [15,17] and biogenic facies mainly constituted of benthic foraminifera [18–20] or coralline red algae [11,16,21–23].

These studies highlighted the occurrence of precious habitats, such as *Posidonia oceanica*, coralligenous and rhodolith/maërl beds. Rhodolith beds are marine communities dominated by free-living, non-geniculate coralline red algae that grow with different morphologies. In this view, the term maërl refers to a kind of rhodolith bed dominated by heavily calcified free-living marine red algae with branched thalli that grow unattached, usually with no articulated joints between segments. In particular, maërl beds are subject to protection measures and the two most common maërl-forming species, *Phymatolithon calcareum* and *Lithothamnion corallioides*, are currently included in the Annex V of the EC Habitats Directive [24–26]. Moreover, they are relevant for their capability to store carbon dioxide CO₂ [27], which is known to be a potent greenhouse gas contributing to global warming. Today, information regarding the real potential of coralline algae to mitigate the effect of increasing anthropogenic CO₂, as well as that regarding their capacity for carbon storage, are still scarce [27–29].

The Pontine Archipelago seabed is peculiar as it is characterized by a complex distribution of siliciclastic, carbonate and mixed siliciclastic-carbonate sediments [30]. In wide sectors of the shelf, the sedimentation is mainly intrabasinal and made up of foraminifera, bryozoans, mollusks, echinoderms and coralline algae. In the infralittoral and circalittoral zones, [15] different facies and sedimentary processes are distinguished. In the infralittoral zone, erosional processes on the rocky shoreline produce lithoclasts and volcanoclastic deposits that are reworked by wave-induced near-shore currents (e.g., longshore currents, rip currents). In the lower circalittoral zone, the prolific production by photic biota (coralline red algae) ends, while skeletal remains of the aphotic environment mix with pelagic sediments characterized by low carbonate content [15]. Regarding benthic foraminifera, [18,19] recognized three assemblages within seabed sediment: the shallowest assemblage (20–150 m water depth) is dominated by *Asterigerinata mamilla*, *Lobatula lobatula* and *Rosalina bradyi*, which at these water depths live as epifaunal taxa on biodetrital circalittoral sediments; the *Cassidulina carinata* assemblage is reported at intermediate depths (100–250 m wd); finally, the deepest assemblage is dominated by *Uvigerina mediterranea* and *Bulimina marginata* (200–380 m wd). The rhodolith morphologies and their distribution around the Pontine Islands were investigated by [11], which distinguished three groups: the unattached, monospecific branches, the small compact “prâlines” and the vacuolar “boxwork”. More recently, [16] identified two carbonate facies between 40 and 100 m wd: the “calcareous algae facies” (40–70 m wd) and the “carbonate matrix facies” (70–100 m wd). Despite abundant literature regarding the modern-seabed sedimentation and foraminiferal assemblages of Pontine Archipelago, stratigraphic and paleoenvironmental studies are rare (e.g., [31,32]). A relationship between rhodolith facies and Holocene sea-level rise in four cores recovered at the Pontine Archipelago shelf break was found by [31], whereas [10,33] investigated events of hardground formation during the Plio-Pleistocene to Holocene record.

In the framework of a project dedicated to the Quaternary paleoenvironmental evolution of the Pontine Archipelago, the aim of this study is to investigate the succession of different paleoenvironments recorded by two sediment cores, collected off Ponza Island, by means of the benthic foraminiferal and rhodoliths assemblages. This has been conducted using the information derived by benthic foraminifera, both taking into account knowledge on their distribution in the recent sediments [18,19]. Moreover, the identification of coralline red algae present along the cores has been used to validate the environmental considerations derived from micropaleontological analysis.

2. Study Area

The Pontine Archipelago is a typical example of a Mediterranean island in terms of climate, oceanography and environments. It consists of five major islands that may

be divided into two groups, Ponza, Palmarola and Zannone (western group) and the Ventotene and Santo Stefano islands (eastern group), located about 30 km off the Italian peninsula (central Tyrrhenian Sea, Italy; Figure 1a). The western group represents the emergent part of a large structural high deeply affected by the Plio-Pleistocene extensional tectonics and volcanic activity [34–36]). These islands mainly consist of submarine and subordinate subaerial volcanic products that erupted during the Plio-Pleistocene, with emplacement of rhyolites and trachytes [37–39].

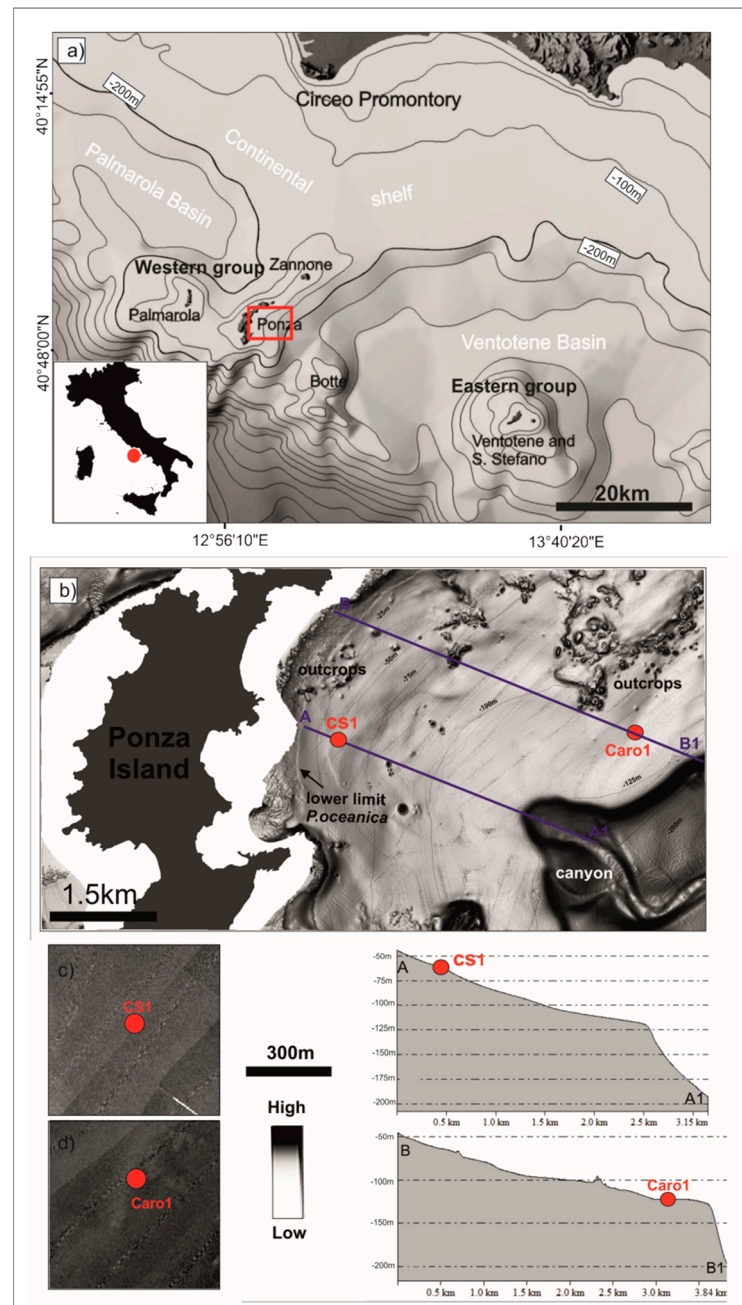


Figure 1. (a) Pontine Archipelago and sampling area (red rectangle); (b) shaded relief map of the Ponza Island offshore, showing the main geomorphologic features and the cores location (red dots); (c,d) multibeam derived backscatter signatures of the seafloor texture observed surrounding the cores, and bathymetric cross-sections showing the seafloor profiles reported as blue lines in Figure 1b.

The Plio-Pleistocene geological evolution leads to the formation of a narrow (2–8 km) and morphologically complex insular shelf characterized by the occurrence of several mor-

phological highs and thin post-Last Glacial Maximum (LGM) deposits. The main deposits are located in the outer shelf-shelf break sector (ca. 100–150 m water depth) and are characterized by sandy sediments, forming prograding wedge-shaped lithosomes (submerged depositional terraces, sensu [40]) formed during the last forced regression-lowstand phases. These deposits surround the Pontine Archipelago, and their formation has been related to high-energy events (storm waves) during the last glacial period [40]. This hypothesis seems to be confirmed by the occurrence of high percentages of glauconitised tests of shallow-water benthic foraminifera (e.g., *Asterigerinata*, *Elphidium* and *Lobatula* [18,19]), which are likely related to the LGM lowstand sea level [10].

Locally, large depressions associated with hydrothermal activity host widespread bacterial mats [41–43] and very peculiar foraminiferal associations [44,45].

Due to the large distance from the Italian coastline as well as the absence of rivers, the shelf seabed is largely characterized by sandy bioclastic sedimentation, as well as by accumulation of volcanoclastic sand produced by coastal erosion in the inner shelf [30,46]. The shelf break is well defined and lies at water depth ranging between 105 and 160 m. The continental slope is characterized by muddy hemipelagic sedimentation and instability processes, especially in the SW sector, connecting the shelf to the Vavilov abyssal Plain [47].

In particular, the shore sector of Ponza Island is mainly characterized by rocky cliffs, locally interrupted by small pocket beaches. The cliffs are affected by intense erosional processes causing their retreatment [30]. On the shelf, the main seafloor sediments are volcanoclastic sands and gravels in the infralittoral zone; bioclastic sands and gravels, consisting of coralline red algae, foraminifera, bryozoans, molluscs and echinoderms in the upper circalittoral zone; and skeletal grains and planktonic foraminifera in the lower circalittoral zone [15].

In the infralittoral zone, *Posidonia oceanica* meadows occur from very shallow water to 38–40 m [17,20,48,49].

3. Materials and Methods

3.1. Geophysical Data

Geophysical data (bathymetry and backscatter) were acquired during the research cruise “MagicIlgag0910” carried out on November 2009 onboard R/V Maria Grazia using Kongsberg EM 3002D (300 kHz, Kongsberg Maritime, Kongsberg, Norway). Sparkler-high-resolution single-channel profiles were acquired during the research cruise “Eleonora 2003” onboard R/V Urania.

Bathymetric data were post-processed with the software Caris Hips and Sips 8.1.7 (Teledyne CARIS, Fredericton, NB Canada), and the backscatter was processed through the Geo-Coder tool. High-resolution digital elevation model (DEM) was produced (cell size 2 m) in order to analyze the surface morphology. Backscatter mosaic with 1 m pixel-resolution was produced to analyze the areal variability of seafloor sediments.

High-resolution seismic data were processed and analyzed using GeoSuite AllWorks (Geo Marine Survey Systems, Rotterdam, The Netherlands) and Kingdom Suite software (version 8.8, IHS Markit, London, UK). These data were used to characterize the seismostratigraphic setting of the study area.

3.2. Sediment Samples

Two cores (CS1 and Caro1) were collected off Ponza Island during the research cruises “Urania 2001” and “Urania 2004”, by a gravity corer on board the R/V Urania. CS1 (218 cm length) was recovered at 60 m water depth (wd) and Caro1 (69 cm length) at 122 m wd (Figure 1b).

The lithological description of the cores was carried out at the time of cores sampling. A total of 32 samples (generally consisting of a 1 cm thick sediment slice) were collected generally every 10 cm: 25 samples from the core CS1 and 7 from the core Caro1 (Figure 2). In the levels in which rhodoliths >1 cm were present, the sample thickness was 2 cm.

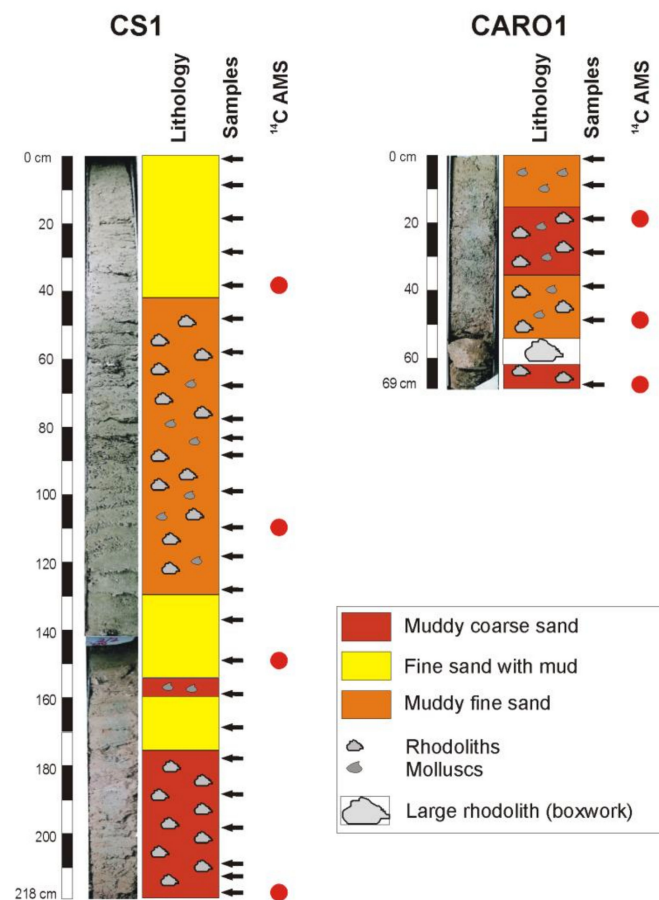


Figure 2. Lithological scheme of the studied cores, with samples (black arrows) and position of radiocarbon-dated levels (red dots).

In the laboratory, the sediment was wet-sieved through a 125 μm mesh and then dried at 60 $^{\circ}\text{C}$. As the sediment was generally abundant, washing residues were split with a microsplitter, and at least 300 benthic foraminifera with well-preserved tests from each sample were handpicked and counted using a binocular microscope [50]. Concomitant counts of planktonic specimens were performed to calculate plankton percentages as $P/(P + B)\%$, in which P is the number of planktonic foraminifera and B is the number of benthic foraminifera in each sample. This ratio is normally considered an indicator of bathymetry [51]. Moreover, the sediment of each sample was sorted under a stereomicroscope in order to pick up the thalli of the coralline red algae present in the, samples and both the algae with entire thalli and algae with fragmented thalli were considered. Then, the algal thalli were separated according to the prevailing morphology, splitting them into the two main morphotypes: unattached branched thalli and prâlines. Then, each fraction was weighed using a precision scale in order to estimate the relative abundance of the algal morphotypes in each portion of sediment. In addition, the species were classified by using Scanning Electron Microscopy (SEM) to identify the skeletal microstructures, and the algal taxa were classified according to [52]. However, the analysis was carried out on the prevailing morphotypes and not on the single species. In fact, according to [11], on the basis of the occurrence of the different growth forms of corallinaceans it is possible to reconstruct the prevailing hydrodynamic conditions. Benthic foraminifera were classified at genus level according to [53]. Their species identification was also based on [54–56]. In order to delineate in detail the assemblage structure, the following parameters were calculated for each sample: the α -Fisher index [57], which is a relationship between the number of species and the number of specimens in each assemblage; the Shannon index [58,59], which takes into account both the number of species and the distribution of individuals among species

and is commonly used as an index of diversity; and the percentage of dominance [60], which is the highest percentage abundance of foraminiferal species in a sample. The diversity indices were calculated by using the PAST (version 3.25, Natural History Museum, University of Oslo, Oslo, Norway)—Palaeontological Statistics data analysis package [61].

The Q-mode Hierarchical Cluster Analysis (HCA) was performed on foraminiferal assemblages using SPSS (version 13.0, IBM, NY, USA) statistical software. The statistical analysis on foraminifera was restricted to the 17 species that were more abundant than 5% in at least one sample. Infrequent taxa (<5% relative abundance) with insignificant effects on the formation of major groups were omitted [62,63]. Consequently, the cluster analysis was performed using a matrix of 17 species and 32 samples. The Ward method was used as the amalgamation rule, and the Squared Euclidean distance as a similarity measurement [64]. The Q-mode HCA classified the samples into clusters, including samples with similar foraminiferal composition.

3.3. Radiocarbon Dates

A total of seven radiocarbon dates (AMS) by Accelerator Mass Spectrometry were performed at the CEDAD (Laboratory of the Department of Engineering Innovation of the University of Salento, Italy), with a 3-MV Tandemron accelerator manufactured by High Voltage Engineering Europa, Amersfoort, The Netherlands. The analyses were carried out on well-preserved and autochthonous tests of benthic foraminifera from four samples of core CS1 and three samples of core Caro1. In order to facilitate comparisons with other studies, data were expressed as instrumental ages (^{14}C AMS dates) and as calibrated ages (Table 1). The calibrated ages were derived applying the program CALIB Radiocarbon Calibration 7.1 (Queen's University of Belfast, Belfast, Northern Ireland, UK) [65]. To calculate the ΔR (reservoir age) for include local effects, two sites were selected from the Marine Reservoir Correction Database of CALIB: the first in the central Tyrrhenian Sea and the second in the Gulf of Naples. The calculated weighted mean ΔR values was 50, with a standard deviation of 18. The calibrated age ranges were reported in years BP and referred to 2σ .

Table 1. Radiocarbon data available for cores CS1 and Caro1.

Cores/Samples	Radiocarbon ^{14}C Age (yr BP)	Calibrated ^{14}C Age (yr BP, 2σ)
CS1		
38 cm	2014 \pm 45	1519 \pm 134
108 cm	4712 \pm 55	4918 \pm 148
148 cm	7431 \pm 55	7831 \pm 125
218 cm	9024 \pm 55	9672 \pm 168
Caro1		
20 cm	10399 \pm 75	11470 \pm 287
50 cm	11702 \pm 75	13119 \pm 190
69 cm	13771 \pm 65	16012 \pm 223

4. Results

4.1. Seabed Morphology and Seismo-Stratigraphic Evidences

The two core samples were recovered on the insular shelf located in the eastern sector of Ponza Island (Figure 1b). The shallower core (CS1) was collected at 60 m wd, in an area characterized by a relatively smooth morphology. Upslope at about 40 m wd, the lower limit of the *P. oceanica* meadow occurs. A cluster of small outcrops (average height of 3 m) is present toward the north, at a water depth varying from 30 to 50 m (Figure 1b). Backscatter data show a seafloor characterized by homogeneous-medium backscatter intensity (Figure 1c).

The deeper core (Caro1) was recovered at 122 m wd close to the shelf break (Figure 1b). In this sector, the seabed has a smooth morphology and lower slope gradient (Figure 1b).

In addition, several small circular outcrops are present (Figure 1b). The backscatter data show a seafloor characterized by heterogeneous-medium backscatter intensity (Figure 1d).

The subsurface structure of the study area was imaged by high-resolution seismic profile EXb crossing the insular shelf between 30 and 200 m wd. It shows the occurrence of a prograding unit resting above a seaward dipping unconformity (U2 in Figure 3). Above the prograding unit, a thin (<10–15 m thick) unit, thinning toward the shelf break, is present, separated by a seaward dipping unconformity (U1 in Figure 3). According to previous interpretations (e.g., [30]), the prograding unit can be related to lowstand-forced regression deposits, whereas the thin unit can be ascribed to postglacial deposits formed after the LGM.

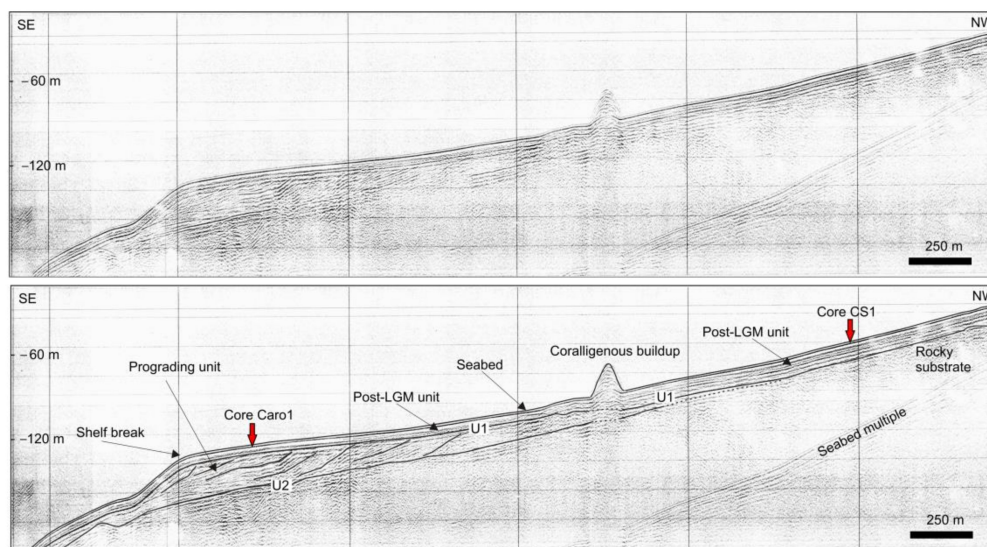


Figure 3. Uninterpreted (upper panel) and interpreted (lower panel) sparker seismic profile (A-A1 in Figure 1b) across the western Pontine shelf with an indication of location of sediment cores CS1 and Caro1 (projected).

Core Caro1 recovered deposits from the distal part of postglacial deposits. In contrast, Core CS1, which is located in the inner shelf, recovered the proximal part of these deposits.

4.2. Lithology and Sediment Composition

The lithology of the core CS1 is represented mainly by coarse to fine clayey sands (Figure 2). From the bottom (218 cm) to 176 cm muddy coarse sand rich in rhodoliths was found: in particular, between the bottom core and 205 cm rhodolith fragments centimeters in size were recognized. The interval from 176 to 160 cm was characterized by fine sand with mud, followed by a level (160 to 154 cm) of muddy coarse sand with bivalve fragments. Successively, from 154 to 130 cm, fine sand with mud was found again. Hence, muddy fine sands were present between 130 and 40 cm, where millimetric bioclastic levels (with mollusks and rhodoliths) were recognized. Finally, fine sand with mud characterized the interval from 40 cm to the top.

The core Caro1 consists of muddy coarse sand with abundant rhodoliths from the bottom to 62 cm (Figure 2). Between 62 and 55 cm core-depth, a very big rhodolith (9 × 8 cm boxwork) was recognized. From 55 to 34 cm, muddy fine sand containing abundant rhodolith and mollusk fragments was found. From 34 to 15 cm, a muddy coarse sand with abundant bivalves and rhodoliths was present. Finally, between 15 cm and the top, muddy fine sand rich in small mollusk fragments was found.

4.3. Benthic Foraminifera

The conservation status of foraminiferal tests is generally good, and consequently, between 301 and 372 benthic foraminifera were counted and classified in each sample. A total of 186 species belonging to 86 genera were identified (Supplementary Table S1). The

samples are generally well diversified, without great differences between the two cores in terms of diversity indices and percentage of dominance (Table 2). Seventeen species show a relative abundance $\geq 5\%$ in at least one sample, but only five species have a frequency $>10\%$ in at least one sample: *Asterigerinata mamilla*, *Cassidulina carinata*, *Lobatula lobatula*, *Quinqueloculina stelligera* and *Rosalina bradyi* (Table 2; Figure S1). The relative abundances along the cores of 17 benthic foraminiferal species utilized for statistical analysis are shown in Figures 4 and 5.

Table 2. Range and median values of species number, α -Fisher index, Shannon index, percentage of dominance, P/(P + B)% and the five more abundant species ($>10\%$) calculated for each core separately and globally.

Summary of Sample Characteristics	CS1			Caro1			Total (CS1 + Caro1)		
	Min	Max	Median	Min	Max	Median	Min	Max	Median
species number	41	65	52	48	61	53	41	65	52
α -Fisher index	12.66	25.16	17.79	15.51	22.39	18.39	12.66	25.16	17.79
Shannon index	2.99	3.59	3.26	3.17	3.54	3.32	2.99	3.59	3.30
Dominance%	9.4	29.1	18.8	12.8	21.1	19.2	9.4	29.1	18.9
P/(P + B)%	1.5	15.4	5.6	6.3	29.5	17.3	1.5	29.5	7.4
<i>A. mamilla</i>	9.4	29.1	18.8	1.9	16.3	9.5	1.9	29.1	16.3
<i>C. carinata</i>	0.0	2.0	0.6	0.3	15.5	4.5	0.0	15.5	0.9
<i>L. lobatula</i>	5.9	14.4	8.8	6.3	21.1	19.2	5.9	21.1	9.0
<i>Q. stelligera</i>	0.0	10.3	1.6	0.0	3.7	1.6	0.0	10.3	1.6
<i>R. bradyi</i>	1.6	10.0	4.0	0.9	4.6	1.9	0.9	10.0	3.8

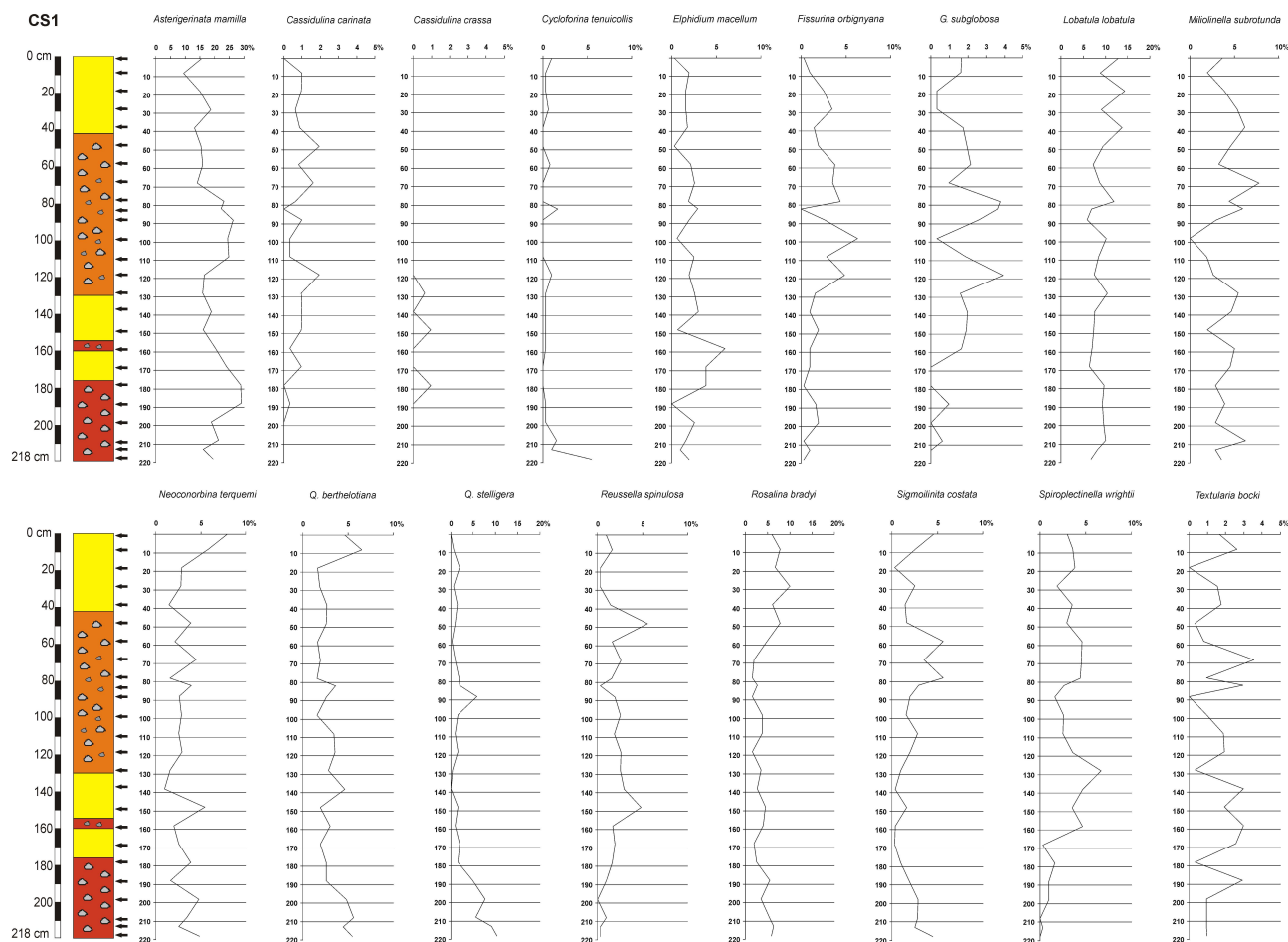


Figure 4. Relative abundance along the core CS1 of 17 benthic foraminiferal species utilized for statistical analysis.

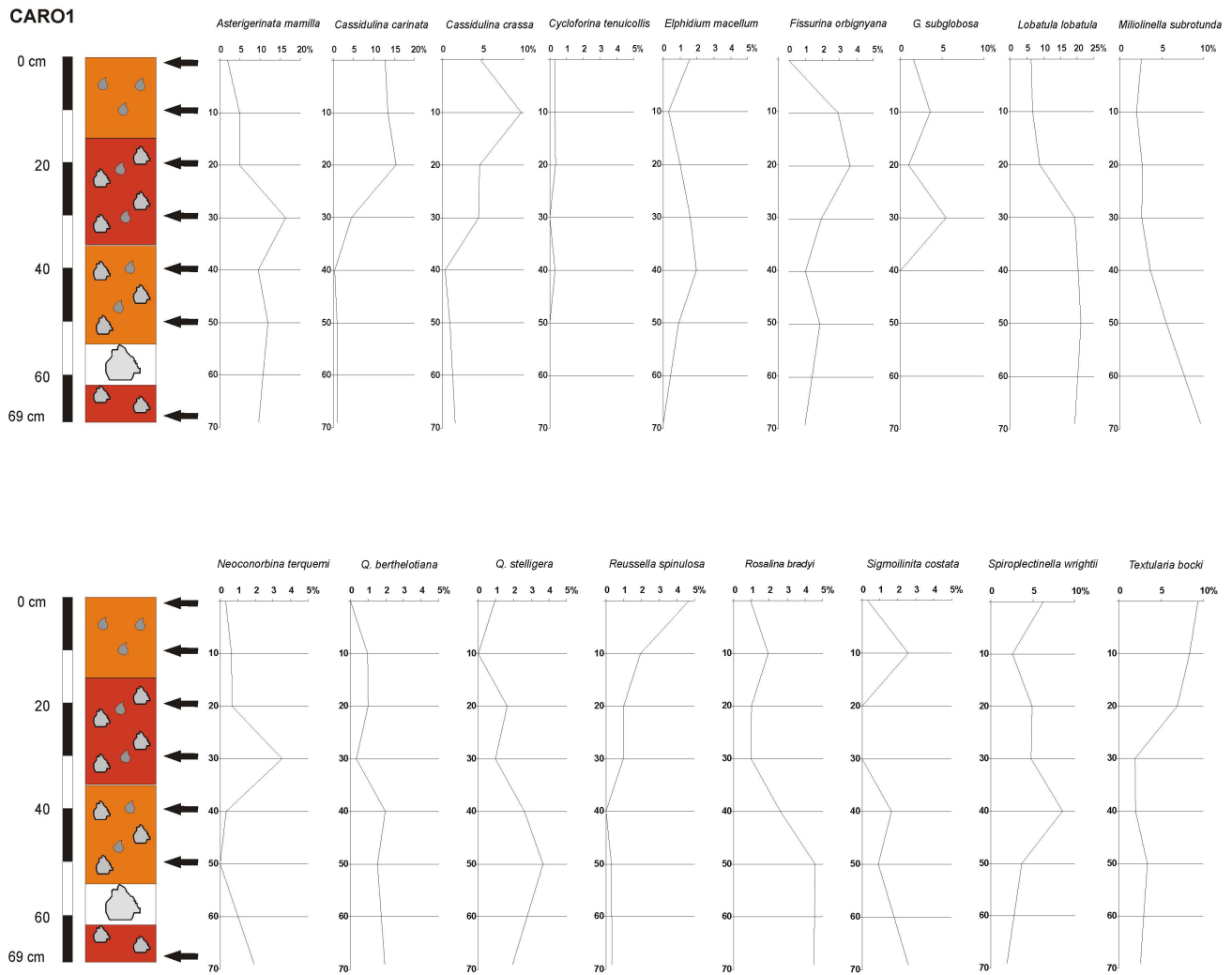


Figure 5. Relative abundance along the core Caro1 of 17 benthic foraminiferal species utilized for statistical analysis.

The P/(P + B)% ratio ranges from very low to high values, with significant differences between the two cores (Table 2). Along the CS1 core, it shows generally low values (maximum 15.4%), whereas it ranges from low to high values (up to 29.5%) in the Caro1 core. The highest percentages are at the upper part of Caro1 core, from 30 cm to the top (17.3–29.5%).

The Q-mode HCA grouped the analyzed samples into clusters, characterized by distinct foraminiferal assemblages reflecting different ecological conditions and helpful to reconstruct the paleoenvironmental evolution of the studied record. The resulting dendrogram contains three main clusters (A, B and C; Figure 6).

Cluster A is characterized by the dominance of *A. mamilla* and is present in 14 samples of CS1 core, from the bottom to 158 cm, 138 cm, and finally 108–178 cm (Figure 7). *Lobatula lobatula* and *Q. stelligera* are other typical species. The values of diversity indices are the lowest recognized, whereas the values of dominance are the highest (Table 3).

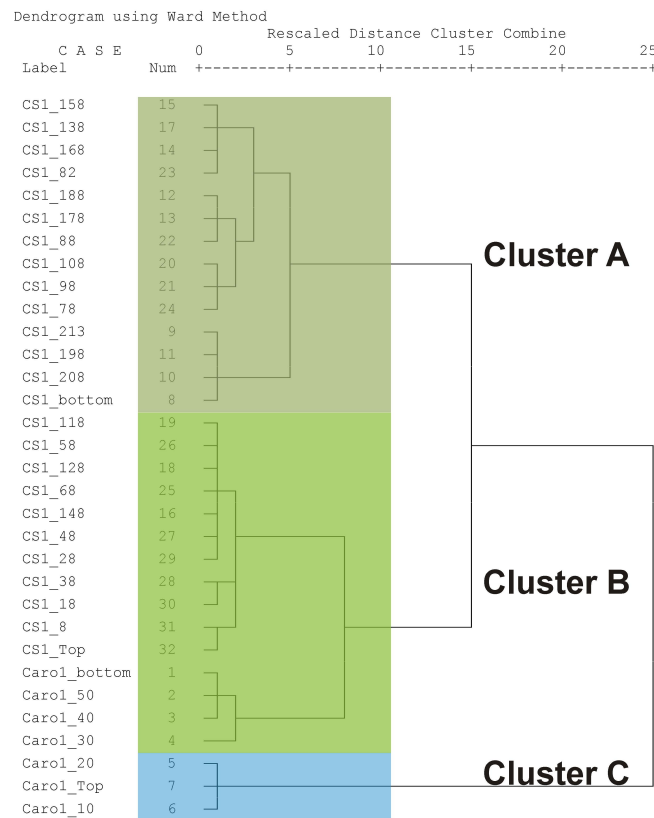


Figure 6. Dendrogram of Q-mode hierarchical cluster analysis of the samples, based on the relative abundance of species >5% (Cluster A: *A. mamilla* assemblage; Cluster B: *A. mamilla* and *L. lobatula* assemblage; Cluster C: *C. carinata* assemblage).

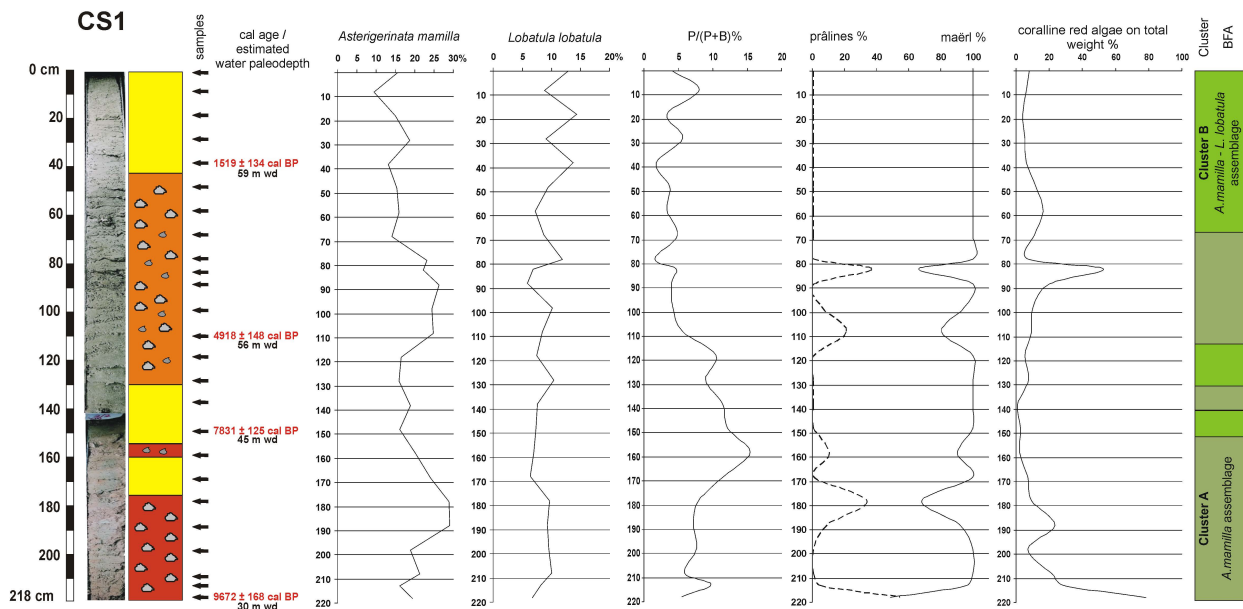


Figure 7. Summary of main data of core CS1: lithology; calibrated radiocarbon dating (yr BP); estimated water paleodepth (according to the sea-level rise curve of [66]); distribution of most abundant benthic foraminiferal species along the core (*Asterigerinata mamilla* and *Lobatula lobatula*); P/(P + B)%; prālines and maërl abundances; percentage of coralline red algae on total weight; distribution of clusters recognized from Q-mode HCA (cluster A: dark green; cluster B: light green) and relative benthic foraminiferal assemblages (BFA).

Table 3. Main features of 3 clusters: dominant species, accompanying species, species number, α -Fisher index, Shannon index, percentage of dominance and P/(P + B)%.

Cluster	Values	A	B	C
Dominant species		<i>A. mamilla</i> (16.2–29.1%)	<i>A. mamilla</i> (9.4–18.7%) and <i>L. lobatula</i> (7.3–21.1%)	<i>C. carinata</i> (12.8–15.5%)
Accompanying species		<i>L. lobatula</i> (5.9–11.9%), <i>Q. stelligera</i> (0–10.3%)	<i>R. bradyi</i> (1.0–10.0%), <i>S. wrighti</i> (1.9–8.5%)	<i>C. crassa</i> (4.6–9.7%), <i>T. bocki</i> (6.9–9.4%), <i>L. lobatula</i> (6.3–8.9%), <i>S. wrighti</i> (2.6–6.3%)
Species number		41–56	48–65	49–61
α -Fisher Index	range	12.66–20.13	15.51–25.16	16.38–22.39
	median	16.98	19.53	22.35
Shannon Index	range	2.99–3.37	3.17–3.59	3.32–3.54
	median	3.23	3.37	3.46
Dominance%	range	16.2–29.1	9.4–21.1	12.8–15.5
	median	22.7	15.9	13.5
P/(P + B)%	range	1.5–16.4	1.7–21.6	17.3–29.5
	median	6.5	6.3	26.6

Cluster B includes samples both of CS1 and Caro1 cores showing a dominance of *A. mamilla* and *L. lobatula*. It is recognisable in the lower part of the Caro1 core (4 samples from the bottom to 25 cm; Figure 8) and in three intervals of the CS1 core (11 samples): around 148 cm, between 128 and 118 cm and, finally, from 68 cm to the top of the core (Figure 7). *Rosalina bradyi* and *Spiroplectinella wrighti* are the only other species showing significant frequencies. The diversity indices show intermediate values as well as the dominance (Table 3).

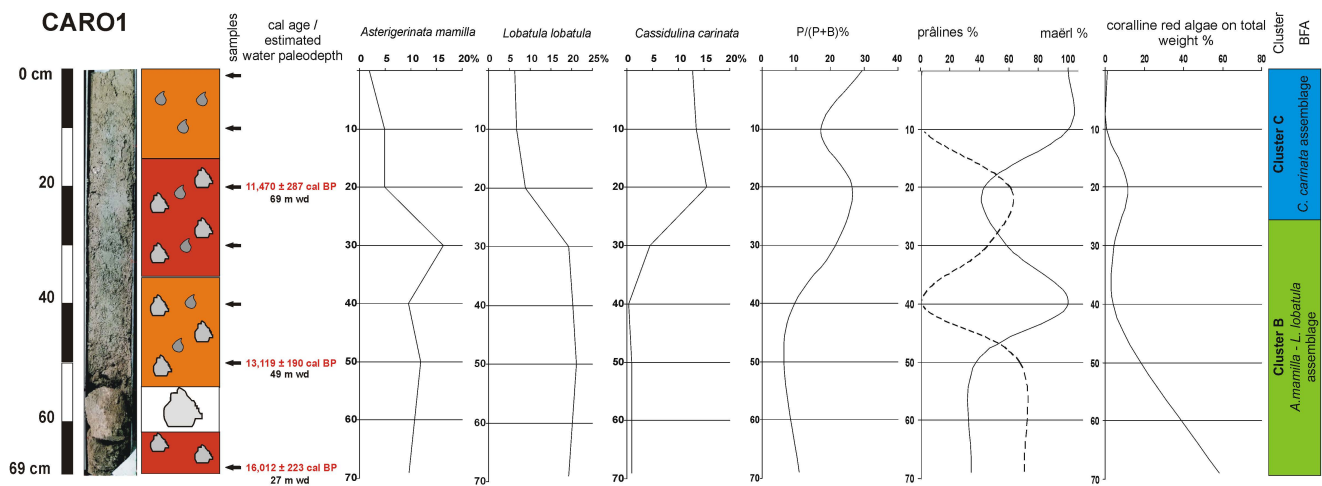


Figure 8. Summary of main data of core Caro1: lithology; calibrated radiocarbon dating (yr BP); estimated water paleodepth (according to the sea-level rise curve of [66]); distribution of most abundant benthic foraminiferal species along the core (*Asterigerinata mamilla*, *Lobatula lobatula* and *Cassidulina carinata*); P/(P + B)%; prâlines and maërl abundances; percentage of coralline red algae on total weight; distribution of clusters recognized from Q-mode HCA (cluster B: light green; cluster C: light blue) and relative benthic foraminiferal assemblages (BFA).

The small cluster C groups only three samples, from 25 cm to the top-core of Caro1 (Figure 8), in which *C. carinata* prevails. *Cassidulina crassa*, *Textularia bocki*, *L. lobatula* and *S. wrighti* are accompanying species. The diversity indices show the highest values, whereas the percentage of dominance is generally low (Table 3).

The samples belonging to clusters A and B show generally low values of P/(P + B)% ratio (Figures 7 and 8; Table 3). On the contrary, in the samples grouped into cluster C P/(P + B)% the ratio reaches the highest values (Figure 8; Table 3).

4.4. Coralline Red Algae

The quantitative analysis shows that at the bottom of core CS1 (Figure 7; Supplementary Table S2), the percentage of coralline red algae on total weight is the highest of the whole core (78.2%) and decreases in the five subsequent samples (7.3–28.4%). Along the successive interval between 168 and 138 cm, they are generally scarce (0.9–7.2%). An increase is evident in the interval from 138 to 98 cm (5.1–10.3%) and more and more at 88–82 cm core-depth, where they reach percentages of 20.2–52.6%. Then, between 78 and 48 cm, the coralline red algae show a decreasing frequency (7.2–16.4%) and become scarce to the top (3.8–8.0%). In the same way, the coralline red algae are very abundant at the bottom of core Caro1 (58.2%), decreasing significantly along the upper part (4.0–18.5%), and almost disappear in the two top samples (0.6–1.0%) (Figure 8; Supplementary Table S2).

The qualitative analysis of the core sediments reveals a conspicuous presence of fossil-unattached coralline algae (Corallinales, Rhodophyta) in the growth form of branched thalli and prâlines (sensu [11]). The branched morphotype consists of unattached branches, whereas prâlines form mainly consist of encrusting-warty, lumpy and fruticose thalli (sensu [22]). The branched thalli were widely predominant in the investigated samples.

It was possible to identify the main species occurring in the sediment cores: the great abundance of the collected specimens belonged to the species *Phymatolithon calcareum* (Pallas) Adey et McKibbin but was well represented also in the other branched species *Lithothamnion corallioides* (P. Crouan and H. Crouan) and *Lithothamnion valens* Foslie; this species association is consistent with the habitat *Phymatolitho-Lithothamnetum corallioidis* Giaccone, 1965, a sciaphilous facies widespread in the Mediterranean Sea [67]. Less abundant were *Lithophyllum racemus* (Lamarck) Foslie and *Lithothamnion minervae* Basso, species characterized by a typical prâlines growth form (Figure S2). It was not possible to determine the epiphytes grew on the bigger thalli due to a wide loss of pigmentation and erosion of the epithallus.

Both the core CS1 and Caro1 are characterized by large fluctuations in the coralline algae abundances, although a general increasing trend downward along the cores can be recognized. The branched thalli, attributable to the maërl-forming species, such as *P. calcareum* and *L. corallioides*, were the dominant growth form in both the investigated cores. In addition, the branched morphotype abundances generally increase upward along the cores, whereas prâlines increase toward the bottom of the cores (Figures 7 and 8; Supplementary Table S2).

More in detail, in the core CS1, the branched thalli were the most abundant growth form in almost all the investigated samples of sediment ($93.5 \pm 9.1\%$ of the total coralline algae). From the top to 78 cm, the only morphology recorded in the sampled rhodoliths consists of unattached branched thalli (Figure 7). It must be noted that the percentage of rhodoliths on the total sediment weight was quite low, with values ranging from 6.1 to 16.4%. At 82 cm depth, an increase was recorded in prâlines with max. size of 1.2 cm in the growth form of lumpy and fruticose thalli (33.9% of the total sampled coralline algae) belonging mainly to the species *L. minervae* and *L. racemus*. This sample also showed an increase in the percentage of rhodoliths on the total sediment weight reaching 52.6% of the total value. From 88 to 168 cm depth, a consistent increase was again recorded in the branched thalli, although the percentage in weight was not high. At 178 cm depth, the prâlines' morphology increased (31.5%), with max. 0.8 cm size.

From 188 to 213 cm depth, the trend showed again a dominance of the branched morphotype. The bottom interval was the only sample that showed a dominance of the prâlines growth form (51.1%) with max. 1.5 cm size. It is necessary to specify that in the deeper samples, from 208 cm depth to the bottom, a marked increase was recorded in the relative weight of the thalli on the total sediment weight, with a peak on the bottom (78.2%), in correspondence with the decrease in the maërl growth form. As recorded in the 82 cm depth sample, also in this case, the prâlines grew up in lumpy and fruticose thalli.

The core Caro1 measured 69 cm from the top to the bottom and also in this case the branched thalli were the dominant growth form, although with lower mean values

($67.7 \pm 27.7\%$) compared to CS1. However, the values varied consistently, not showing a clear trend (Figure 8). In fact, from the top to 10 cm depth, only very few unattached branched thalli were observed (respectively 1.0 and 0.6% of the total sediment weight), whereas at 20 and 30 cm depth was recorded an increase of the prâlines in the encrusting-warty growth form (respectively 56.8 and 41.6%). In these last samples, the percentage of rhodoliths showed an increase (respectively 11.7 and 4.4% of the total sediment weight). Moreover, in the following samples a fluctuating trend was recorded, with a decrease in the abundance of unattached thalli (100% at 40 cm depth, 37.7% at 50 cm depth and 34.6% at the bottom); on the other hand, these samples showed an increase of the percentage of rhodoliths on the total sediment weight (respectively 4%, 18.5% and 58.2%). In fact, in this sample, the prâlines growth form showed high values at 20 and 50 cm depth and on the bottom surface (respectively 56.8, 62.3 and 65.4%).

However, mean values in terms of relative weight of the thalli on the total sediment weight were similar in both the cores Caro1 and CS1 (respectively 14.5 ± 11.0 and $14.1 \pm 13.9\%$), with a peak again on the bottom interval (respectively 78.2 and 58.2%). Moreover, clear evidence of praline levels (e.g., at centimeter scale) cannot be observed from the visual description of these cores. Differently results from the relative abundance of pralines (Figures 7 and 8) would suggest the occurrence of intervals with relatively higher abundance of pralines.

4.5. Age Model and Sedimentation Rates

The ^{14}C AMS datings indicate that the sediments of core CS1 were deposited during the last ~9600 yr BP, whereas the core Caro1 was deposited during the last 16,000 yr BP. The age model is provided by four and three ^{14}C AMS datings for CS1 and Caro1 cores, respectively (Table 1). Assuming invariant sedimentation rates between two successive radiocarbon dates, it is possible to estimate the sedimentation rates along the cores, which result as low for core CS1 and very low for core Caro1. In core CS1, the highest sedimentation rate has been recognized from the bottom to 148 cm (0.038 cm/yr); up-core, it decreases up to 108 cm (0.014 cm/yr) and increases between 108 and 38 cm (0.021 cm/yr) and toward the top (0.025 cm/yr). Along core Caro1, the sedimentation rate is very low from the bottom to 50 cm (0.007 cm/yr); it increases up to 0.018 cm/yr between 50 and 20 cm, while at the top of core it decreases up to 0.002 cm/yr.

5. Discussion

5.1. Ecological Considerations Based on Benthic Foraminiferal Assemblages

Based on Q-mode CA, the three clusters A, B and C, corresponding to three benthic foraminiferal assemblages, were identified (Figure 6). Two clusters (A and B) are similar regarding the composition at least regarding the main species and their lifestyle, while the third (C) is different, reflecting different ecological conditions. In general, the diversity indices of these clusters show values similar or higher than recent foraminiferal assemblages recognized in the Pontine Archipelago [19], indicating normal marine environments with good species diversity. Along the cores, diversity indices show an increase from the bottom to the top in both the cores, following the change from cluster A to B in CS1 core and from cluster B to C in Caro1.

Cluster A is characterized by the prevalence of *A. mamilla* with relatively high percentages. *Lobatula lobatula* and *Q. stelligera* are the other species having significant frequencies. *Asterigerinata mamilla* was reported as very abundant from the infralittoral zone, especially on vegetated seabed [20,68–70] but also from circalittoral detrital bottoms [18,19,55,71–73]. *Lobatula lobatula* shows a similar distribution in the Mediterranean area: it is abundant from the infralittoral zone, especially on *Posidonia* meadows [20,69,71,74–77], but it is also present from circalittoral detrital bottoms [18,19,55]. *Quinqueloculina stelligera* is frequent in the infralittoral zone, mainly on coarse sandy or vegetated bottoms [18,55,70], but, in general, all miliolids are commonly described as linked to a vegetated seafloor [69,78].

Cluster B is dominated by taxa typical of infralittoral/upper circalittoral bottoms such as *A. mamilla* and *L. lobatula*. *Rosalina bradyi* and *S. wrighti* are other significant components. Similar foraminiferal assemblages dominated by *A. mamilla*, *L. lobatula* and *Rosalina bradyi* are typical of Recent Mediterranean infralittoral vegetated bottoms (e.g., [18–20,69,70,77,79–81]). Nevertheless, these taxa are described also as epifaunal suspension feeders, living permanently or temporarily attached to coarse substrates, such as bioclastic sands and gravels [7,59]. The same assemblage is present in the modern seafloor of the Pontine Archipelago [18,19] and, precisely, between 30 and 100 m wd, where the bottom is characterized by coarse biodetritral sediment.

The differences between clusters A and B do not seem related to different ecological preferences of dominant and accompanying species: they are generally adapted to live as epifauna attached to coarse substrate. The differences can be found in the values of diversity indices and percentages of dominance (Table 3). The diversity is rather lower in cluster A (α -Fisher Index: 12.66–20.13) than in cluster B (α -Fisher Index: 15.51–25.16), while the dominance shows an opposite trend: 16.2–29.1% and 9.4–21.1%. These data indicate relatively more stressed (or worse) conditions for cluster A, probably due to high current activities.

Cluster C groups only three samples from 25 cm to the top of the Caro1 core, dominated by *C. carinata*. This species is typical of circalittoral and bathyal muds [55,68,75,82]. In the modern sediments of the Pontine Archipelago, the *C. carinata* assemblage is reported in the lower circalittoral zone (100–200 m; [18,19]).

As a whole, both cluster A (*A. mamilla*) and cluster B (*A. mamilla* and *L. lobatula*) indicate bathymetries ranging between 30 and 100 m. Nevertheless, these two clusters can be related to biodetritral circalittoral sediments, because the recent benthic foraminiferal communities found in the *Posidonia* meadows near Ponza Island (<50 m wd) are characterized by the dominance of *L. lobatula* and *R. bradyi* with high abundances of symbiont-bearing species *Peneroplis pertusus* [20]. On the contrary, cluster C (*Cassidulina carinata*) indicates clearly a deeper environment (currently, 100–200 m wd).

5.2. Environmental Conditions Required for the Free-Living Red Algae Growth

The coralline red algae assemblages recognized along the cores can occur both in temperate and tropical waters with a vertical distribution usually limited to the sciaphilous habitats in the lower infralittoral zone and in the circalittoral zone. It must be noted that the Mediterranean maërl beds show much higher biodiversity compared with Atlantic maërl beds [25,52,83]. Moreover, rhodoliths are considered coastal ecosystem engineers, and both their morphology and bed distribution are highly affected by the coastal environment. In this view, fossil free-living coralline algae can be considered as palaeoindicators of the past environmental and hydrodynamic conditions [84].

Although temperature and light are basic environmental factors known to control their distribution, also the water energy affects significantly both morphology and growth form as well as the sedimentation rate [85–87]. In fact, if the water flow is too slow, rhodoliths can be smothered by silt, but in the case of a too fast water flow, rhodoliths can be susceptible to breakage [88]. In Brittany (France), rhodolith beds are found in areas where mean current velocity ranges from 0.02 to 0.73 m/s, with the lowest percentage of rhodolith cover (<59% covered) occurring in areas of water velocities exceeding 0.50 m/s [89]. In addition, rhodoliths volume and branching density generally decrease with water depth [90].

It is well known that the observed species are typical of sciaphilous habitats and can be found within a relatively wide bathymetric range, from the infralittoral to the circalittoral zone (usually from 20 to 40 m depth; 65 m depth for *Lithophyllum racemus*) [52,83,91]. Off western Pontine islands, rhodoliths can be found between 40 and 100 m wd [11,15,16,22]. They are a growing in situ species that accumulates to form assemblages frequently associated with submarine bedforms (e.g., ripple marks or dunes) [92].

The collected taxa are consistent with the results reported in previous studies in the same geographical area [86] and the branched thalli, attributable to the maërl-forming

species, such as *P. calcareum* and *L. coralloides*, were the dominant growth forms. These species usually constitute the *Phymatolitho-Lithothamnietum coralloidis* Giaccone association, 1965, a facies typical of the circalittoral zone, but also developed in the lower infralittoral zone. This sciaphilous habitat is assumed to have fairly narrow ecological requirements, and its distribution seems to be in close connection to specific controlling environmental factors [67].

From considering the hydrodynamic and sedimentological requirements of the sampled branched coralline species, it emerges that those are all taxa typical of habitat characterized by relatively high energy environments, characterized by vigorous hydrodynamism, laminar bottom currents, clean water, coarse sand mixed with muddy sediments and bottom instability [11,52,67,93]. On the other hand, prâlines-shaped thalli grow preferentially in the biocenosis of sand and gravel (S.G.C.F.) under strong and turbulent bottom currents [52,94]. In addition, according to the laboratory studies carried out by [25], the maërl-forming species *P. calcareum* seems to be deleteriously affected by the presence of fine sediment with a high organic matter content.

The multibeam data acquired in the area surrounding the sediment cores do not show evidence of the action of vigorous bottom currents able to rework the seabed in bedforms (e.g., ripples, dunes) at present. Nonetheless, according to [22], the absence of a significant muddy component in bioclastic sediments, especially for the Caro1, would support the occurrence of moderate bottom currents at the seafloor, and this can support the occurrence of rhodoliths.

5.3. Paleoenvironmental Reconstruction

The bottom of CS1 core is dated 9672 ± 168 cal BP, corresponding to a sea level about 30 m lower than the current one, if plotted on the sea-level rise curve related to “Italia site 7” (Fondi area) ([66]; Figure 9). Consequently, the bathymetric variation along the core would be limited from 30 (bottom) to 60 m (top-core). From the bottom to 150 cm (between 9672 ± 168 and 7831 ± 125 cal BP), the sediments are dominated by cluster A (*A. mamilla*; Figure 7). In this interval, two peaks of rhodoliths are present at the bottom and at 178 cm. From 148 to 68 cm, a fluctuation is present between cluster A and cluster B (*A. mamilla* and *L. lobatula*). In particular, two other levels with abundant rhodoliths are recognized at 108 and 82 cm, always corresponding to cluster A. Although the rhodoliths are not abundant in all the samples of cluster A, in which *A. mamilla* dominates, a link between rhodoliths content and *A. mamilla* can be supposed. This relationship could be due to the occurrence of bottom currents, in which rhodoliths grow. On the other hand, the present sediments of Pontine Archipelago characterized by abundant *A. mamilla* are also rich in rhodoliths [18,19]. Around 60 cm, and up to the top-core, cluster B is definitely established, and rhodolith frequencies decrease. At 38 cm depth-core (1519 ± 134 cal BP), the CS1 core reaches a water depth of 59 m, which is very similar to the current water depth (60 m; Figure 9). In general, both these foraminiferal assemblages can be referred to as a recent *A. mamilla*, *L. lobatula* and *R. bradyi* assemblage. It is actually present in these bathymetric range of Pontine Archipelago in areas not covered by *P. oceanica* meadows [18,19]. The presence of these similar benthic foraminiferal assemblages and the relatively few variations in the lithology, together with the stable values of $P/(P + B)\%$, confirm that there are no interesting large bathymetrical variations in the CS1 core (Figure 7).

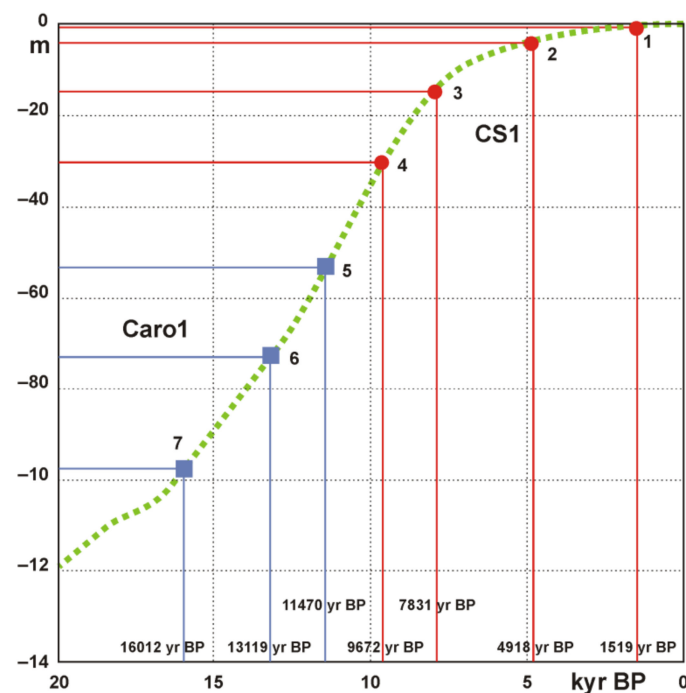


Figure 9. Eustatic and glacio-hydro-isostatic predictions for Italian sites for the past 20,000 years (redrawn and simplified from [66]). Samples of the cores CS1 (red dots) and Caro1 (blue squares) are plotted on the curve (1: CS1_38 cm; 2: CS1_108 cm; 3: CS1_148 cm; 4: CS1_bottom; 5: Caro1_20 cm; 6: Caro1_50 cm; 7: Caro1_bottom).

On the contrary, a clear bathymetric change is recorded in the Caro1 core. From the bottom to 30 cm core-depth, cluster B (*A. mamilla* and *L. lobatula* assemblage actually present between 30 and 100 m wd) is recognized, whereas above and up to the top, it is replaced by cluster C (*C. carinata*), typical of the 100–200 m range (Figure 8). In this core, the relationship between *A. mamilla* abundance and rhodolith content is not clear as in core CS1. According to the radiocarbon date (16012 ± 223 cal BP) plotted on the sea-level rise curve of [66], the bottom was deposited at a water depth approximately 95 m lower than the actual one (Figure 9). Considering the water depth of coring (122 m), the bottom of Caro1 was deposited at a water depth of 27 m, during the final phase of the last glacial lowstand. Between 62 and 55 cm (i.e., in the time interval from $16,012 \pm 223$ to $13,119 \pm 190$ cal BP), a very big rhodolith (boxwork) is present. This could testify to an active carbonate deposition during a cold period (close to the LGM), which was rarely described (e.g., [95]). The subsequent sea level rise involves the increase of the water depth that at 20 cm ($11,470 \pm 287$ cal BP) approximates 70 m (cluster C). The top 10 cm probably corresponds to the highstand phase that occurred along the Tyrrhenian margin 6000 years ago. This basin deepening is also confirmed by the sharp transition from coarser to finer lithology and by the $P/(P + B)\%$ shift (Figure 8). It is low (6.3–10.9%) until 40 cm core-depth and subsequently strongly increases (17.3–29.5%), reaching typical values of these water depths [19].

Overall, foraminifera assemblages indicate that core Caro1 records a well-defined deepening of the paleoenvironment. This is also mirrored by the coralline algal abundance, which decreases upward along the core (Figure 8), consistently to what was observed in other sectors of the Pontine Archipelago [31].

Both the core CS1 and Caro1 are characterised by large fluctuations in the coralline algae abundances that might indicate variable hydrodynamic conditions and/or input of finer sediment.

Interestingly, for both the bottom cores, the radiocarbon dates plotted on the sea-level rise curve (“Italia site 7” [66]) provide a paleobathymetry of about 30 m. This water depth is compatible with the recognized benthic foraminiferal assemblage (clusters A and B), and

with dispersed rhodoliths in the Pontine Archipelago (30–100 m; [15,16]). The occurrence of extensive rhodolith on the present-day shelf [22] and the long depositional record of rhodoliths make this place a relevant natural site to study the present and past conditions of carbonate production. The occurrence of a possible boxwork and the relatively higher abundance of rhodoliths older than 13,000 years in the basal part of core Caro1 suggest the possible presence of an active carbonate factory at Pontine Archipelago, for a longer time than known so far (10,000 years, according to [31]). In addition, the finding of rhodolite-rich sediment in the postglacial stratigraphic record represents a relevant aspect, as they play a relevant role in carbon cycling and sequestration [27].

6. Conclusions

In this study, two sediment cores collected off Ponza Island (central Tyrrhenian Sea) were analyzed. Paleontological data (benthic foraminifera and coralline red algae), integrated with geophysical data and radiocarbon dates, have led to a paleoenvironmental reconstruction of the last 16,000 yr BP in the Pontine Archipelago. Sediments from core Caro1 recorded an evident deepening succession, with a transition from a basal rhodolith-rich biodetritic coarse sand to the surface coralline-barren silty sand. This water depth increasing is also reflected in the increase of the $P/(P + B)\%$ and in the change of the benthic foraminiferal assemblages, from cluster B (*A. mamilla* and *L. lobatula*; infralittoral-upper circalittoral zones) to a deeper-water assemblage cluster C (*C. carinata*; lower circalittoral zone). These assemblages are similar to those found at different water depths in the present seafloor of the Pontine Archipelago. A slightly different situation was recorded by core CS1 that is located at shallower depth (middle shelf), in which the water-depth increases from the bottom to the top is probably limited to a few tens of meters. Nevertheless, the decrease in rhodolith content from the bottom to the top is recognisable also in this core. Regarding the benthic foraminiferal content, it is rather constant along the core with an alternation between cluster A (*A. mamilla*) and cluster B (*A. mamilla* and *L. lobatula*). These assemblages are both referable to the infralittoral-upper circalittoral zones and show the presence of dominant species having similar ecological preferences. A difference between these two clusters can be found in the species diversity, which is lower in cluster A, indicating relatively more stressed conditions.

Overall, this study extends the rhodolith record in the Pontine Archipelago at a time between 16,000 and 13,000 years BP (occurrence of a big rhodolith in the lower part of the core Caro1) compared to what has been observed so far (around 10,000 years BP). Consequently, it is possible to consider that a mixed siliciclastic-carbonate sedimentation was already active during the post-LGM.

Supplementary Materials: The following are available online at <https://www.mdpi.com/article/10.3390/geosciences11040179/s1>, Figure S1: Scanning electron micrographs of some significant benthic foraminiferal species recognized in the CS1 and Caro1 cores. Scale bar = 100 μm : 1. *Spiroplectinella wrighti*, side view; 2. *Textularia bocki*, side view; 3. *Quinqueloculina stelligera*, side view; 4. *Cassidulina carinata*, side view; 5. *Asterigerinata mamilla*, spiral view; 6. *Asterigerinata mamilla*, umbilical view; 7. *Rosalina bradyi*, spiral view; 8. *Rosalina bradyi*, umbilical view; 9. *Lobatula lobatula*, spiral view; 10. *Lobatula lobatula*, umbilical view, Figure S2: Different growth forms detected in the sampled rhodoliths. Scale bar = 1 cm: a. small branched thalli; b. larger branched thalli; c. fragmented branched thalli; d. prâlines, Table S1: Relative abundances of the foraminiferal species recognized in each sample of CS1 and Caro1 cores, Table S2: Quantitative analysis of coralline red algae.

Author Contributions: V.F., L.D.B. prepared the samples and performed the foraminiferal analyses. A.B., L.A. prepared the samples and performed the rhodoliths analyses. F.L.C. collected both core samples and multibeam and seismic data. M.I., E.M. made the analyses and interpretation of multibeam (bathymetry and backscatter) and seismic data. V.F., M.I. contributed to the editing of the present versions of the manuscript. All authors participated in the writing of the present version of the manuscript. All authors have read and agreed to the published version of the manuscript.

Funding: This study was funded by the “Progetto di Ricerca di Università 2019—La risposta adattativa delle faune bentoniche in ambienti estremi attuali e fossili” (L. Di Bella).

Institutional Review Board Statement: Not applicable.

Informed Consent Statement: Not applicable.

Data Availability Statement: Not applicable.

Acknowledgments: We would like to thank all the officers, crew, and technicians of the R/Vs Maria Grazia and Urania for their precious work and their help during onboard activities. We also acknowledge the anonymous reviewers for their valuable comments and suggestions.

Conflicts of Interest: The authors declare no conflict of interest. The funders had no role in the design of the study; in the collection, analyses, or interpretation of data; in the writing of the manuscript; or in the decision to publish the results.

References

1. Nelson, C.S. An introductory perspective on non-tropical shelf carbonates. *Sed. Geol.* **1988**, *60*, 3–12. [[CrossRef](#)]
2. Tropeano, M.; Spalluto, L. Present-day temperate-type carbonate sedimentation on Apulia shelves (southern Italy). *Geoacta* **2006**, *5*, 129–142.
3. James, N.P. The cool-water carbonate depositional realm. In *Cool-Water Carbonates*; James, N.P., Clarke, J.A.D., Eds.; SEPM Special Publications: Broken Arrow, OK, USA, 1997; Volume 56, pp. 1–20.
4. Betzler, C.; Brachert, T.C.; Nebelsick, J. The warm temperate carbonate province. A review of the facies, zonations, and delimitations. *Cour. Forsch. Senckenberg* **1997**, *201*, 83–99.
5. Pérès, J.M.; Picard, J. Nouveau manuel de bionomie marine benthique de la Mer Méditerranée. *Rec. Trav. Stat. Mar. Endoume* **1964**, *31*, 5–138.
6. Carannante, G.; Esteban, M.; Milliman, J.D.; Simone, L. Carbonate lithofacies as paleolatitude indicators: Problems and limitations. *Sediment. Geol.* **1988**, *60*, 333–346. [[CrossRef](#)]
7. Milker, Y.; Schmiedl, G.; Betzler, C.; Römer, M.; Jaramillo-Vogel, D.; Siccha, M. Distribution of recent benthic foraminifera in shelf carbonate environments of the Western Mediterranean Sea. *Mar. Micropaleontol.* **2009**, *73*, 207–225. [[CrossRef](#)]
8. Martorelli, E.; Falese, F.; Chiocci, F.L. Overview of the variability of Late Quaternary continental shelf deposits of the Italian peninsula. In *Continental Shelves of the World: Their Evolution During the Last Glacio-Eustatic Cycle*; Chiocci, F.L., Chivas, A.R., Eds.; Geological Society Memoirs: London, UK, 2014; Volume 41, pp. 171–186.
9. Colantoni, P.; Cremona, G.; Ligi, M.; Borsetti, A.M.; Cati, F. The Adventure Bank (off Southwestern Sicily): A present day example of carbonate shelf sedimentation. *Giorn. Geol.* **1985**, *47*, 165–180.
10. Corselli, C.; Basso, D.; Garzanti, E. Paleobiological and sedimentological evidence of Pleistocene/Holocene hiatuses and ironstone formation at the Pontian islands shelfbreak (Italy). *Mar. Geol.* **1994**, *117*, 317–328. [[CrossRef](#)]
11. Basso, D. Deep rhodolith distribution in the Pontian Islands, Italy: A model for the paleoecology of a temperate sea. *Palaeogeogr. Palaeoclim. Palaeoecol.* **1998**, *137*, 173–187. [[CrossRef](#)]
12. Toscano, F.; Sorgente, B. Rhodalgae-Bryomol temperate carbonates from the Apulian Shelf (Southeastern Italy), relict and modern deposits on a current dominated shelf. *Facies* **2002**, *46*, 103–118. [[CrossRef](#)]
13. Lecca, L.; De Muro, S.; Cossellu, M.; Pau, M. I sedimenti terrigeno-carbonatici attuali della piattaforma continentale del Golfo di Cagliari. *Il Quat.* **2005**, *18*, 201–221.
14. Toscano, F.; Vigliotti, M.; Simone, L. Variety of coralline algal deposits (rhodalgae facies) from the Bays of Naples and Pozzuoli (northern Tyrrhenian Sea, Italy). In *Cool-Water Carbonates: Depositional Systems and Palaeoenvironmental Controls*; Pedley, H.M., Carannante, G., Eds.; Geological Society Special Publication: London, UK, 2006; Volume 255, pp. 85–94.
15. Brandano, M.; Civitelli, G. Non-seagrass meadow sedimentary facies of the Pontinian Islands, Tyrrhenian Sea: A modern example of mixed carbonate-siliciclastic sedimentation. *Sediment. Geol.* **2007**, *201*, 286–301. [[CrossRef](#)]
16. Bracchi, V.A.; Basso, D. The contribution of calcareous algae to the biogenic of the continental shelf: Pontian Islands, Tyrrhenian sea, Italy. *Geodiversitas* **2012**, *34*, 61–76. [[CrossRef](#)]
17. Gaglianone, G.; Brandano, M.; Mateu-Vicens, G. The sedimentary facies of *Posidonia oceanica* seagrass meadows from the central Mediterranean Sea. *Facies* **2017**, *63*, 1–21. [[CrossRef](#)]
18. Frezza, V.; Carboni, M.G.; Matteucci, R. Recent foraminiferal assemblages near Ponza Island (Central Tyrrhenian Sea, Italy). *Boll. Soc. Paleontol. Ital.* **2005**, *44*, 155–173.
19. Frezza, V.; Pignatti, J.S.; Matteucci, R. Benthic foraminiferal biofacies in temperate carbonate sediment in the Western Pontine Archipelago (Tyrrhenian Sea, Italy). *J. Foraminifer. Res.* **2010**, *40*, 313–326. [[CrossRef](#)]
20. Frezza, V.; Baldassarre, A.; Gaglianone, G.; Mateu-Vicens, G.; Brandano, M. Mixed carbonate-siliciclastic sediments and benthic foraminiferal assemblages from *Posidonia oceanica* seagrass meadows of the central Tyrrhenian continental shelf (Latium, Italy). *Ital. J. Geosci.* **2011**, *130*, 352–369.

21. Martorelli, E.; D'Angelo, S.; Fiorentino, A.; Chiocci, F.L. Nontropical Carbonate Shelf Sedimentation. The Archipelago Pontino (Central Italy) Case History. In *Seafloor Geomorphology as Benthic Habitat*; Harris, P.T., Baker, E.K., Eds.; Elsevier: Amsterdam, The Netherlands, 2012; pp. 449–456.
22. Sañé, E.; Chiocci, F.L.; Basso, D.; Martorelli, E. Environmental factors controlling the distribution of rhodoliths: An integrated study based on seafloor sampling, ROV and side scan sonar data, offshore the W-Pontine Archipelago. *Cont. Shelf Res.* **2016**, *129*, 10–22. [[CrossRef](#)]
23. Ingrassia, M.; Martorelli, E.; Sañé, E.; Falese, F.G.; Bosman, A.; Bonifazi, A.; Argenti, L.; Chiocci, F.L. Coralline algae on hard and soft substrata of a temperate mixed siliciclastic-carbonatic platform: Sensitive assemblages in the Zannone area (western Pontine Archipelago; Tyrrhenian Sea). *Mar. Environ. Res.* **2019**, *147*, 1–12. [[CrossRef](#)]
24. Council Directive. Council Directive 92/43/EEC of 21 May 1992 on the conservation of natural habitats and of wild fauna and flora. *Off. J. Eur. Communities Legis.* **1992**, *206*, 7–50.
25. Wilson, S.; Blake, C.; Berges, J.A.; Maggs, C.A. Environmental tolerances of free-living coralline algae (maerl): Implications for European marine conservation. *Biol. Conserv.* **2004**, *120*, 279–289. [[CrossRef](#)]
26. Curiel, D.; Rismondo, A.; Falace, A.; Kaleb, S. Affioramenti rocciosi sommersi (tegnùe) e la Rete Natura 2000: Possibili S.I.C. marini per il Nord Adriatico. *Biol. Mar. Mediterr.* **2009**, *16*, 103–106.
27. Van der Heijden, L.H.; Kamenos, N.A. Reviews and syntheses: Calculating the global contribution of coralline algae to total carbon burial. *Biogeosciences* **2015**, *12*, 6429–6441. [[CrossRef](#)]
28. Hill, R.; Bellgrove, A.; Macreadie, P.I.; Petrou, K.; Beardall, J.; Steven, A.; Ralph, P.J. Can macroalgae contribute to blue carbon? An Australian perspective. *Limnol. Oceanogr.* **2015**, *60*, 1689–1706. [[CrossRef](#)]
29. Macreadie, P.I.; Jarvis, J.; Trevathan-Tackett, S.M.; Bellgrove, A. Seagrasses and macroalgae: Importance, vulnerability and impacts. In *Climate Change Impacts on Fisheries and Aquaculture: A Global Analysis*; Phillips, B.F., Pérez-Ramírez, M., Eds.; Wiley-Blackwell: Hoboken, NJ, USA, 2017; pp. 729–770.
30. Chiocci, F.L.; Martorelli, E. *Carta Geologica D'Italia Alla Scala 1:50.000. F° 412. Borgo Grappa Isole Ponziane*; Geologico d'Italia: Catania, Italy, 2018; p. 413.
31. Basso, D.; Morbioli, C.; Corselli, C. Rhodolith facies evolution and burial as a response to Holocene transgression at the Pontian Islands shelf break. In *Cool-Water Carbonates: Depositional Systems and Palaeoenvironmental Controls*; Pedley, H.M., Carannante, G., Eds.; Geological Society Special Publication: London, UK, 2006; Volume 255, pp. 23–34.
32. Ragazzola, F.; Caragnano, A.; Basso, D.; Schmidt, D.N.; Fietzke, J. Establishing temperate crustose early Holocene coralline algae as archives for palaeoenvironmental reconstructions of the shallow water habitats of the Mediterranean Sea. *Palaeontology* **2020**, *63*, 155–170. [[CrossRef](#)]
33. Conti, M.A.; Girasoli, D.E.; Frezza, V.; Conte, A.M.; Martorelli, E.; Matteucci, R.; Chiocci, F.L. Repeated events of hardground formation and colonisation by endo-epilithozoans on the sediment-starved Pontine continental slope (Tyrrhenian Sea, Italy). *Mar. Geol.* **2013**, *336*, 184–197. [[CrossRef](#)]
34. De Rita, D.; Funicello, R.; Pantosti, D.; Salvini, F.; Sposato, A.; Velonà, M. Geological and structural characteristics of the Pontine Islands (Italy) and implications with the evolution of the tyrrhenian margin. *Mem. Soc. Geol. Ital.* **1986**, *36*, 55–65.
35. Marani, M.; Zitellini, N. Rift structures and wrench tectonics along the continental slope between Civitavecchia and C. Circeo. *Mem. Soc. Geol. Ital.* **1986**, *35*, 453–457.
36. Bellucci, F.; Lirer, L.; Munno, R. Geology of Ponza, Ventotene and Santo Stefano islands (with a 1:15,000 scale geological map). *Acta Vulcanol.* **1999**, *11*, 197–222.
37. Conte, A.M.; Dolfi, D. Petrological and geochemical characteristics of Plio-Pleistocene Volcanics from Ponza Island (Tyrrhenian Sea, Italy). *Mineral. Pet.* **2002**, *74*, 75–94.
38. Cadoux, A.; Pinti, D.L.; Aznar, C.; Chiesa, S.; Gillot, P.Y. New chronological and geochemical constraints on the genesis and geological evolution of Ponza and Palmarola Volcanic Islands (Tyrrhenian Sea, Italy). *Lithos* **2005**, *81*, 121–151. [[CrossRef](#)]
39. Conte, A.M.; Perinelli, C.; Bianchini, G.; Natali, C.; Martorelli, E.; Chiocci, F.L. New insights on the petrology of submarine volcanics from the Western Pontine Archipelago (Tyrrhenian Sea, Italy). *J. Volcanol. Geotherm. Res.* **2016**, *327*, 223–239. [[CrossRef](#)]
40. Chiocci, F.L.; Orlando, L. Lowstand terraces on Tyrrhenian Sea steep continental slopes. *Mar. Geol.* **1996**, *134*, 127–143. [[CrossRef](#)]
41. Ingrassia, M.; Martorelli, E.; Bosman, A.; Macelloni, L.; Sposato, A.; Chiocci, F.L. The Zannone Giant Pockmark: First evidence of a giant complex seeping structure in shallow-water, central Mediterranean Sea, Italy. *Mar. Geol.* **2015**, *363*, 28–51. [[CrossRef](#)]
42. Martorelli, E.; Italiano, F.; Ingrassia, M.; Macelloni, L.; Bosman, A.; Conte, A.M.; Beaubien, S.E.; Graziani, S.; Sposato, A.; Chiocci, F.L. Evidence of a shallow water submarine hydrothermal field off Zannone Island from morphological and geochemical characterization: Implications for Tyrrhenian Sea Quaternary volcanism. *J. Geophys. Res. Solid Earth* **2016**, *121*, 8396–8414. [[CrossRef](#)]
43. Rastelli, E.; Corinaldesi, C.; Dell'Anno, A.; Tangherlini, M.; Martorelli, E.; Ingrassia, M.; Chiocci, F.L.; Lo Martire, M.; Danovaro, R. High potential for temperate viruses to drive carbon cycling in chemoautotrophy-dominated shallow-water hydrothermal vents. *Environ. Microbiol.* **2017**, *19*, 4432–4446. [[CrossRef](#)] [[PubMed](#)]
44. Di Bella, L.; Ingrassia, M.; Frezza, V.; Chiocci, F.L.; Martorelli, E. The response of benthic meiofauna to hydrothermal emissions in the Pontine Archipelago, Tyrrhenian Sea (central Mediterranean Basin). *J. Mar. Syst.* **2016**, *164*, 53–66. [[CrossRef](#)]

45. Di Bella, L.; Ingrassia, M.; Frezza, V.; Chiocci, F.L.; Pecci, R.; Bedini, R.; Martorelli, E. *Spiculosphon oceana* (Foraminifera) a new bio-indicator of acidic environments related to fluid emissions of the Zannone Hydrothermal Field (central Tyrrhenian Sea). *Mar. Environ. Res.* **2018**, *136*, 89–98. [[CrossRef](#)]
46. Martorelli, E.; Chiocci, F.L.; Civitelli, G.; Chimenz, C.; Ventura, G.; Altobelli, C.; Balocco, A.; Bosman, A.; Cassata, L.; Raspagliosi, M. Mid-latitude carbonate sedimentation on a volcanic island shelf (Pontine Islands, Tyrrhenian Sea). In Proceedings of the Abstracts Volume of 2nd IGCP464 Annual Conference, San Paulo/Cananea, Brasil, 30 August–3 September 2002; p. 1.
47. Chiocci, F.L.; Martorelli, E.; Bosman, A. Cannibalization of a continental margin by regional scale mass wasting: An example from the central Tyrrhenian Sea. In *Submarine Mass Movements and Their Consequences*; Locat, J., Mienert, J., Eds.; Kluwer Academic Publishers: Dordrecht, The Netherlands, 2003; pp. 409–416.
48. Ardizzone, G.D.; Belluscio, A. Le praterie di Posidonia oceanica lungo le coste laziali. In *Il Mare del Lazio. Oceanografia Fisica e Chimica, Biologia e Geologia Marina, Clima Meteorologico, Dinamica dei Sedimenti e apporti Continentali*; Università degli Studi di Roma “La Sapienza”, Regione Lazio, Assessorato Opere e Reti di Servizi e Mobilità: Roma, Italy, 1996; pp. 194–217.
49. Mateu-Vicens, G.; Brandano, M.; Gaglianone, G.; Baldassarre, A. Seagrass-meadow sedimentary facies in a mixed siliciclastic-carbonate temperate system in the Tyrrhenian Sea (Pontinian Islands, western Mediterranean). *J. Sediment. Res.* **2012**, *82*, 451–463. [[CrossRef](#)]
50. Schönfeld, J.; Alve, E.; Geslin, E.; Jorissen, F.; Korsun, S.; Spezzaferri, S. Members of the FOBIMO group, 2012. The FOBIMO (FORaminiferal Bio-MONitoring) initiative—towards a standardized protocol for soft-bottom benthic foraminiferal monitoring studies. *Mar. Micropaleontol.* **2012**, *94*, 1–13. [[CrossRef](#)]
51. Van der Zwaan, G.J.; Jorissen, F.J.; De Stigter, H.C. The depth dependency of planktonic/benthic foraminiferal ratios: Constraints and applications. *Mar. Geol.* **1990**, *95*, 1–16. [[CrossRef](#)]
52. Bressan, G.; Babbini, L. Corallinales del mar Mediterraneo: Guida alla determinazione. *Biol. Mar. Mediterr.* **2003**, *10*, 237.
53. Loeblich, A.R., Jr.; Tappan, H. *Foraminiferal Genera and their Classification*; Van Nostrand Reinhold Company: New York, NY, USA, 1987; p. 970.
54. Cimerman, F.; Langer, M.R. Mediterranean Foraminifera. *Acad. Sci. Artium Slov.* **1991**, *30*, 1–118.
55. Sgarrella, F.; Moncharmont Zei, M. Benthic Foraminifera of the Gulf of Naples (Italy): Systematics and autoecology. *Boll. Soc. Paleontol. Ital.* **1993**, *32*, 145–264.
56. Fiorini, F.; Vaiani, S.C. Benthic foraminifera and transgressive-regressive cycles in the Late Quaternary subsurface sediments of the Po Plain near Ravenna (Northern Italy). *Boll. Soc. Paleontol. Ital.* **2001**, *40*, 357–403.
57. Fisher, R.A.; Corbet, A.S.; Williams, C.B. The relationship between the number of species and the number of individuals in a random sample of an animal population. *J. Anim. Ecol.* **1943**, *12*, 42–58. [[CrossRef](#)]
58. Murray, J.W. *Ecology and Paleocology of Benthic Foraminifera*; Longman Scientific and Technical: New York, NY, USA, 1991; p. 312.
59. Murray, J.W. *Ecology and Applications of Benthic Foraminifera*; Cambridge University Press: Cambridge, UK, 2006; p. 426.
60. Walton, W.R. Recent foraminiferal ecology and paleoecology. In *Approaches to Paleocology*; Imbrie, J., Newell, N.D., Eds.; John Wiley: New York, NY, USA, 1964; pp. 151–237.
61. Hammer, Ø.; Harper, D.A.T.; Ryan, P.D. PAST: Paleontological statistics software package for education and data analysis. *Palaeontol. Electron.* **2001**, *4*, 1–9.
62. Kovach, W.L. Multivariate methods of analyzing paleoecological data. *Paleontol. Soc. Spec. Publ.* **1987**, *3*, 72–104. [[CrossRef](#)]
63. Kovach, W.L. Comparisons of multivariate analytical techniques for use in Pre-Quaternary plant paleoecology. *Rev. Palaeobot. Palynol.* **1989**, *60*, 255–282. [[CrossRef](#)]
64. Parker, W.C.; Arnold, A.J. Quantitative methods of analysis in foraminiferal ecology. In *Modern Foraminifera*; Sen Gupta, B.K., Ed.; Kluwer Academic Publishers: Dordrecht, The Netherlands, 1999; pp. 71–89.
65. Stuiver, M.; Reimer, P.J. Extended ¹⁴C database and revised CALIB radiocarbon calibration program. *Radiocarbon* **1993**, *35*, 215–230. [[CrossRef](#)]
66. Lambeck, K.; Antonioli, F.; Anzidei, M.; Ferranti, L.; Leoni, G.; Scicchitano, G.; Silenzi, S. Sea level change along the Italian coast during the Holocene and projections for the future. *Quat. Int.* **2011**, *232*, 250–257. [[CrossRef](#)]
67. Giaccone, G.; Giaccone, T.; Catra, M. Maërl or free calcareous Algae (Melobesiae) facies (association with Lithothamnion corallioides and Phymatolithon calcareum: Phymatolitho-Lithothamnietum corallioidis Giaccone 1965). In *Priority Habitats According to the SPA/BIO Protocol (Barcelona Convention) Present in Italy. Identification Sheets*; Relini, G., Giaccone, G., Eds.; Italian National Research Council: Rome, Italy, 2009; Volume 16, pp. 122–126.
68. Jorissen, F.J. The distribution of benthic foraminifera in the Adriatic Sea. *Mar. Micropaleontol.* **1987**, *12*, 21–48. [[CrossRef](#)]
69. Langer, M.R. Recent epiphytic foraminifera from Vulcano (Mediterranean Sea). *Rev. Paléobiol. Vol. Spéc.* **1988**, *2*, 827–832.
70. Langer, M.R. Epiphytic foraminifera. *Mar. Micropaleontol.* **1993**, *20*, 235–265. [[CrossRef](#)]
71. Jorissen, F.J. Benthic Foraminifera from the Adriatic Sea; principles of phenotypic variation. *Utrecht Micropaleontol. Bull.* **1988**, *37*, 1–174.
72. Moufii-El-Houari, L.; Ambroise, D.; Mathieu, R. Distribution of recent Benthic Foraminifera of the continental margin of Algeria (Bou-Ismaïl Bay). *Rev. De Micropaléontol.* **1999**, *42*, 315–327. [[CrossRef](#)]
73. Ferraro, L.; Alberico, I.; Lirer, F.; Vallefucio, M. Distribution of benthic foraminifera from the southern Tyrrhenian continental shelf (South Italy). *Rend. Lincei* **2012**, *23*, 103–119. [[CrossRef](#)]

74. Vénec-Peyré, M.T.; Le Calvez, Y. Les Foraminifères épiphytes de l'herbier de Posidonies de Banyuls-sur-Mer (Méditerranée occidentale) étude des variations spatiotemporelles du peuplement. *Cah. Micropaléont.* **1988**, *3*, 21–40.
75. Frezza, V.; Carboni, M.G. Distribution of Recent foraminiferal assemblages near the Ombrone River mouth (northern Tyrrhenian Sea, Italy). *Rev. De Micropaléontol.* **2009**, *52*, 43–66. [[CrossRef](#)]
76. Buosi, C.; Arminot Du Châtelet, E.; Cherchi, A. Benthic foraminiferal assemblages in the current-dominated Strait of Bonifacio (Mediterranean Sea). *J. Foraminifer. Res.* **2012**, *42*, 39–55. [[CrossRef](#)]
77. Benedetti, A.; Frezza, V. Benthic foraminiferal assemblages from shallow-water environments of northeastern Sardinia (Italy, Mediterranean Sea). *Facies* **2016**, *62*, 1–17. [[CrossRef](#)]
78. Ribes, T.; Gracia, M.P. Foraminifères des herbiers de posidonies de la Méditerranée occidentale. *Vie Et Milieu* **1991**, *41*, 117–126.
79. Langer, M.R.; Frick, H.; Silk, M.T. Photophile and sciaphile foraminiferal assemblages from marine plant communities of Lavezzi Islands (Corsica, Mediterranean Sea). *Rev. Paléobiol.* **1998**, *17*, 525–530.
80. Mateu-Vicens, G.; Box, A.; Deudero, S.; Rodríguez, B. Comparative analysis of epiphytic foraminifera in sediments colonized by seagrass *Posidonia oceanica* and invasive macroalgae *Caulerpa* spp. *J. Foraminifer. Res.* **2010**, *40*, 134–147. [[CrossRef](#)]
81. Mateu-Vicens, G.; Khokhlova, A.; Sebastián-Pastor, T. Epiphytic foraminiferal indices as bioindicators in Mediterranean seagrass meadows. *J. Foraminifer. Res.* **2014**, *44*, 325–339. [[CrossRef](#)]
82. Carboni, M.G.; Frezza, V.; Bergamin, L. Distribution of Recent benthic foraminifera in the Ombrone River Basin (Tuscany Continental Shelf, Tyrrhenian Sea, Italy): Relations with fluvial run-off. In *Proceedings in the 1st Italian Meeting on Environmental Micropaleontology*; Cocconeri, R., Galeotti, S., Lirer, F., Eds.; Grzybozsky Foundation Special Publication: Kraków, Poland, 2004; Volume 9, pp. 7–16.
83. Basso, D.; Babbini, L.; Ramos-Esplá, A.A.; Salomidi, M. Mediterranean rhodolith beds. In *Rhodolith/Maerl Beds: A Global Perspective*; Riosmena-Rodríguez, R., Nelson, W., Aguirre, J., Eds.; Springer International Publishing: Cham, Switzerland, 2017; pp. 281–298.
84. Brandano, M.; Vannucci, G.; Mateu-Vicens, G. Le alghie rosse calcaree come indicatori paleoambientali: L'esempio della rampa carbonatica Laziale-Abruzzese (Burdigaliano, Appennino centrale). *Boll. Soc. Geol. Ital.* **2007**, *126*, 55–69.
85. Bosence, D.W.; Pedley, H.M. Sedimentology and palaeoecology of a Miocene coralline algal biostrome from the Maltese islands. *Palaeogeogr. Palaeoclimatol. Palaeoecol.* **1982**, *38*, 9–43. [[CrossRef](#)]
86. Basso, D.; Favaga, P.; Piazza, M.; Vannucci, G. Biostratigraphic, paleobiogeographic and paleoecological implications in the taxonomic review of Corallinaceae. *Rend. Lincei* **1998**, *9*, 201–211. [[CrossRef](#)]
87. Melbourne, L.A.; Denny, M.W.; Harniman, R.L.; Rayfield, E.J.; Schmidt, D.N. The importance of wave exposure on the structural integrity of rhodoliths. *J. Exp. Mar. Biol. Ecol.* **2018**, *503*, 109–119. [[CrossRef](#)]
88. Foster, M.S. Rhodoliths: Between rocks and soft places. *J. Phycol.* **2001**, *37*, 659–667. [[CrossRef](#)]
89. Dutertre, M.; Grall, J.; Ehrhold, A.; Hamon, D. Environmental factors affecting maerl bed structure in Brittany (France). *Eur. J. Phycol.* **2015**, *50*, 371–383. [[CrossRef](#)]
90. Steller, D.L.; Foster, M.S. Environmental factors influencing distribution and morphology of rhodoliths in Bahía Concepción, BCS, México. *J. Exp. Mar. Biol. Ecol.* **1995**, *194*, 201–212. [[CrossRef](#)]
91. Cabioch, J. Le maërl des côtes de Bretagne et le problème de sa survie. *Penn Ar Bed* **1970**, *7*, 421–429.
92. Basso, D.; Babbini, L.; Kaleb, S.; Bracchi, V.; Falace, A. Monitoring deep Mediterranean rhodolith beds. *Aquat. Conserv. Mar. Freshwat. Ecosyst.* **2016**, *26*, 549–561. [[CrossRef](#)]
93. Hall-Spencer, J.M.; Moore, P.G. Scallop dredging has profound, long-term impacts on maerl habitats. *Ices J. Mar. Sci.* **2000**, *57*, 1407–1415. [[CrossRef](#)]
94. Bellan-Santini, D. The Mediterranean benthos: Reflections and problems raised by a classification of the benthic assemblages. In *Mediterranean Marine Ecosystems*; Moraitou-Apostolopoulou, M., Kiortis, V., Eds.; Nato Conference Series; Springer: Boston, MA, USA, 1985; Volume 8, pp. 19–48.
95. Bracchi, V.A.; Basso, D.; Savini, A.; Corselli, C. Algal reefs (Coralligenous) from glacial stages: Origin and nature of a submerged tabular relief (Hyblean Plateau, Italy). *Mar. Geol.* **2019**, *411*, 119–132. [[CrossRef](#)]